PROCEEDINGS OF SCIENCE

Correlation studies on UHECR arrival direction and source candidates with a convolution of magnetic field and mass composition

Ryo Higuchi for the TA collaboration[a,*]

[a] *Astrophysical Big Bang Laboratory (ABBL), RIKEN, 2-1 Hirosawa, Wako, Saitama 351-0198, Japan*

E-mail: ryo.higuchi@riken.jp

Several studies reported the correlation between the arrival directions of ultra-high-energy cosmic rays (UHECRs) and nearby starburst galaxies (SBGs). Auger collaboration (2018, 2022) reported a $\sim 4\sigma$ significance correlation with SBGs, and the Telescope Array (TA) experiment also showed consistent results (TA collaboration 2018). Considering the effects of the magnetic field on UHECR flux would be mandatory to constrain the UHECR source population. We re-investigate the correlation of UHECR arrival direction obtained by the TA and Auger experiments with nearby SBGs. In the analysis, we changed the UHECR flux model from SBGs based on three assumptions: (1) the same flux model as in the Auger collaboration (2022), (2) distance dependence of scattering angle by a turbulent extra-galactic magnetic field, (3) deflection and scattering by the galactic magnetic (GMF) field. For the estimation of the effects of the galactic magnetic (GMF) field, we developed the method to calculate the log-likelihood with the GMF model (Jansson and Farrar 2012ab) and mass composition model (global-spline fit, Dembinski et al. 2017). We confirmed less than 2 and 4 sigma global significance for TA and Auger experiments, respectively. The assumption of scattering by a turbulent extra-galactic magnetic field does not change the significance with order. The current result with GMF is sensitive to mass-composition assumption. In this report, we report the current status of our analysis and discuss the model dependence.

7th International Symposium on Ultra High Energy Cosmic Rays (UHECR2024)
17-21 November 2024
Malargüe, Mendoza, Argentina

*Speaker

 ISSN 1824-8039 . Published by SISSA Medialab.

PoS(UHECR2024)093

1. Introduction

There are reported correlations between UHECR arrival directions and nearby SBGs [1, 4]. The Pierre Auger Observatory (Auger experiment) reported $\sim 4\sigma$ correlation [1] at 39 EeV energy threshold. The Telescope Array (TA) experiment has conducted the same analysis and showed consistent results from the Auger experiment [3]. The joint-analysis working group with the TA and Auger experiments reports 4.7σ significance with full-sky exposure [7].

The correlation studies have some uncertainties and questions, which need to be addressed to constrain the source of UHECR. We focus on three items to be discussed. First, the test in TA experiment [3] did not conduct a global scan and fixed the energy threshold as 43EeV, which is scaled energy from 39 EeV in the Auger experiment. Because the distribution of source candidates and the magnetic field structure are different in the northern and southern hemispheres, it is interesting to compare independent global scans using the TA and Auger datasets. Second, the correlation studies assume simple assumptions: the isotropic scattering by a turbulent magnetic field. The effect by magnetic fields is approximated to be the isotropic scattering with an angular scale parameter θ (scattering angle), which is fixed independently on the source distances. In physical realization, the scattering angle should depend on source distances, described in Section 3.2. Lastly, we need to care about coherent magnetic field deflections. When the effects of coherent magnetic field in the Galaxy (GMF) are dominant, the result of correlation studies significantly changes in both TA and Auger datasets [8].

In this study, we conduct three analyses. First, we describe the dataset and catalog in Section 2. We briefly summarize the maximum log-likelihood method in [4] and our updates with magnetic field models in Section 3. In Section 4.1, we test the global scan for the TA experiment dataset, in the same manner as in Auger analysis [4]. In Section 4.2, we test the modified distance scaling, changing the scattering angle with a physical assumption. In the last part (Section 4.3), we develop a method to calculate correlation with the GMF model.

2. Datasets

We use a 14-year dataset obtained by the TA experiment and public dataset of Pierre Auger Observatory[13]. Due to the difference in the energy spectrum between TA and Auger experiments, we scale energies -4.5% for TA and $+4.5\%$ for Auger datasets. After the energy scaling the TA (Auger) dataset includes 541 (2522) events above 34 EeV. We conduct the energy scan with an energy threshold of 34 EeV to 100 EeV. Following [4], we adapt the SBG catalog in [11]. The example of a flux map in equatorial coordinates can be seen in Figure 1.

3. Method

3.1 Maximum log-likelihood search in previous works

In general, we follow the equations in [4]. In [4] the log-likelihood ratio is written as:

$$TS = 2 \times \sum_{CR} \ln \left(H_1(\mathbf{n_{CR}}) / H_0(\mathbf{n_{CR}}) \right), \tag{1}$$

where H_1 and H_0 indicate the likelihood of the SBG model and isotropic model (null hypothesis), respectively, for each event $n_{\rm CR}$. The likelihood of SBG and isotropic models can be written as

$$H_1(\mathbf{n_{CR}}) = \frac{(1-\alpha)\cdot F_{\rm iso}\cdot\omega(\mathbf{n_{CR}}) + \alpha\cdot F(\mathbf{n_{CR}})\cdot\omega(\mathbf{n_{CR}})}{\sum_{\rm pixel}[(1-\alpha)\cdot F_{\rm iso}\cdot\omega(\mathbf{n}_{\rm pixel}) + \alpha\cdot F(\mathbf{n}_{\rm pixel})\cdot\omega(\mathbf{n}_{\rm pixel})]} \tag{2}$$

and

$$H_0(\mathbf{n_{CR}}) = F_{\rm iso}\cdot\frac{\omega(\mathbf{n_{CR}})}{\sum_{\rm pixel}\omega(\mathbf{n}_{\rm pixel})}, \tag{3}$$

where $F_{\rm iso}$ is isotropic number density ($F_{\rm iso} = \frac{1}{4\pi}$), α represents the anisotropic fraction and $\mathbf{n}_{\rm pixel}$ show the direction of each pixel. We calculate the exposure of each experiment $\omega(\mathbf{n})$ following [12]. The function $F(\mathbf{n})$ represents the total CR flux from each source i:

$$F(\mathbf{n}_{\rm pixel}) = \sum_i w_i f_i(\mathbf{n}_{\rm pixel}), \tag{4}$$

where w_i and f_i represent a relative contribution from each source i and CR flux in von-Mises Fisher representation

$$f_i(\kappa,\mathbf{n}) = \kappa\exp(\kappa\cos\mathbf{n}_i\cdot\mathbf{n})/(4\pi\sinh\kappa), \tag{5}$$

respectively. Following [4], we approximate the κ as $\kappa = \frac{1}{2(1-\cos(\theta))}$ with scattering angle θ. We calculate TS in equation 1 and estimate the best-fit parameters (α,θ) which maximizes TS.

3.2 Analysis with distance scaling

In the actual propagation, the scattering angle θ should be scaled depending on the source distance d_i (distance scaling). We rewrite the CR model flux as

$$\theta^{\rm scaling} = \sqrt{d_i/d_{\rm norm}}\times\theta, \tag{6}$$

where we choose normalization distance $d_{\rm norm}$ to be 3.61 Mpc (M82), which is closest SBG in the catalog. Then the $F(\mathbf{n})$ is calculated as

$$F(\mathbf{n}_{\rm pixel}) = \sum_i w_i f_i^{\rm scaling}(\mathbf{n}_{\rm pixel}) \tag{7}$$

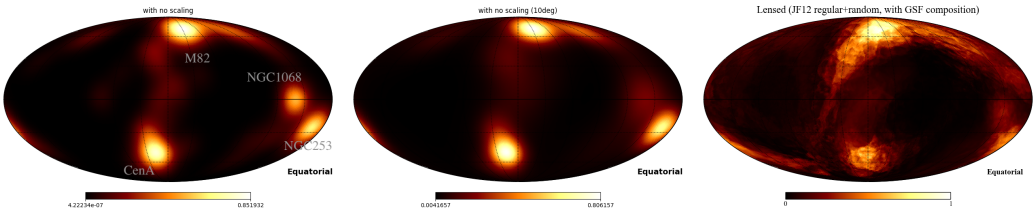

Figure 1: Examples of CR flux map from SBG catalog [11] in equatorial coordinates (scattering angle is fixed to be $\theta = 10\,$deg). From left to right, we show the original flux map, flux map with distance scaling, and GMF lensing, respectively.

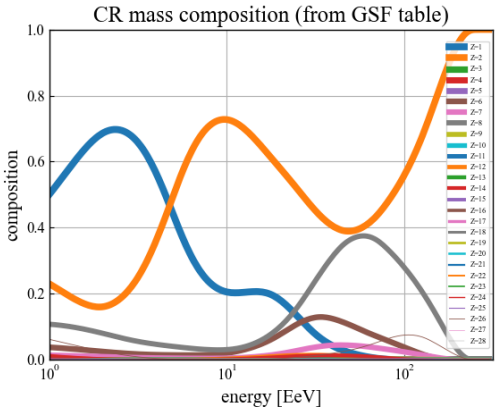

Figure 2: mass composition from GSF fit [6]. Each line represents the probability of charge Z at each energy E

where

$$f_i^{\text{scaling}}(\mathbf{n}_{\text{pixel}}) = \kappa^{\text{scaling}} * \exp(\kappa^{\text{scaling}} \cos \mathbf{n}_i \cdot \mathbf{n})/(4\pi \sinh \kappa^{\text{scaling}}) \tag{8}$$

$$\kappa^{\text{scaling}} = \frac{1}{2(1-\cos(\theta^{\text{scaling}}))}. \tag{9}$$

The calculation of likelihood analysis is the same as Equation 2. In the middle panel of Figure 1, we show an example of the CR flux map with distance scaling. Due to the longer source distances, the flux around NGC1068 and the supergalactic plane is weaker than the original flux map (left).

3.3 Analysis with GMF lensing

3.3.1 mass composition function with GSF fit

To calculate CR model flux with GMF effects, we need to assume the mass (charge) of each CR event. We refer to the Global Spline Fit (GSF) of cosmic rays [6] in the 10 to 300 EeV range (Figure 2). We adopt a mass composition function from the GSF $p(E, Z)$: the probability of charge Z when the CR event has an energy of E.

3.3.2 GMF lensing

We apply GMF lensing with JF12 model [9, 10] with CRPropa 3.2[5]. We call the GMF lensing function $A_{\text{GMF}}(R, F(\mathbf{n}))$ and rewrite H_1 flux. The CR model flux F can be changed as:

$$F^{\text{GMF}}(E, Z, \mathbf{n_{CR}}) = A_{\text{GMF}}(R, F(\mathbf{n_{CR}})) \tag{10}$$

Then we can rewrite H_1 flux to be:

$$H_1(\mathbf{n_{CR}}) = \frac{(1-\alpha)\cdot F_{\text{iso}}\cdot\omega(\mathbf{n_{CR}}) + \alpha\cdot F^{\text{GMF}}(\mathbf{n_{CR}})\cdot\omega(\mathbf{n_{CR}})}{\sum_{\text{pixel}}[(1-\alpha)\cdot F_{\text{iso}}\cdot\omega(\mathbf{n}_{\text{pixel}}) + \alpha\cdot F^{\text{GMF}}(\mathbf{n}_{\text{pixel}})\cdot\omega(\mathbf{n}_{\text{pixel}})]} \tag{11}$$

$$= \frac{(1-\alpha)\cdot F_{\text{iso}}\cdot\omega(\mathbf{n_{CR}}) + \alpha\cdot A_{\text{GMF}}(R, F(\mathbf{n_{CR}}))\cdot\omega(\mathbf{n_{CR}})}{\sum_{\text{pixel}}[(1-\alpha)\cdot F_{\text{iso}}\cdot\omega(\mathbf{n}_{\text{pixel}}) + \alpha\cdot A_{\text{GMF}}(R, F(\mathbf{n_{pixel}}))\cdot\omega(\mathbf{n}_{\text{pixel}})]}. \tag{12}$$

We need to choose a charge Z for each event from mass composition function $p(E, Z)$.

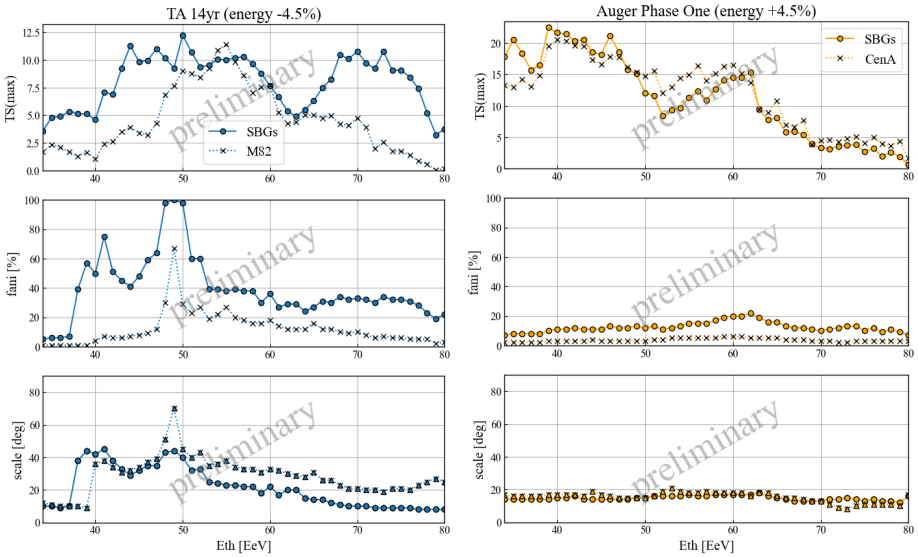

Figure 3: The energy scan results of TS (top), best-fit anisotropic fraction α (middle) and scattering angle θ (bottom). Blue (orange) circles and solid lines show the correlation between the TA (Auger) dataset and the SBG catalog in [11]. Black crosses indicate the correlation between the TA (Auger) dataset and M82 (CenA).

4. Results

4.1 correlation with SBGs in TA and Auger datasets

Figure 3 shows the result of energy threshold scans on TA and Auger datasets. To test the significance of the maximum values of TS, we generate $O(1000)$ MC datasets from the isotropic model. From the TS distribution of the MC datasets, we estimate the p-value and calculate the local significance at each energy threshold. We confirm 4.5σ local maximum significance for the Auger dataset at 39 EeV (after energy scaling), consistent with [4]. The maximum local significance of the TA dataset is 3.2σ at 50 EeV. We conduct a global scan over 34-100 EeV energy thresholds. To derive the global significance, we generate 10, 000 MC datasets over 34-100 EeV energy thresholds, and calculate TS values. After considering the penalty of the scan, we confirm 1.8σ (3.8σ) global significance for the TA (Auger) dataset. The previous report of Auger dataset [4] indicates double peaks in TS (the maximum one is at $\sim$ 40 EeV and another is at $\sim$ 60 EeV.). We can also see another TS peak around 70 EeV in the TA dataset.

We also test the correlation between the datasets and most nearby sources in each exposure. The dotted line in the left (right) panel in Figure 3 shows a correlation between the TA (Auger) dataset and M82 (CenA). The correlations between M82 and the TA dataset show a single peak in TS (at 55 EeV, which corresponds to 57 EeV: an energy threshold from "hotspot" report in [2]), while correlations between the CenA and the Auger dataset show a double peak as in the original report [4]. Although the single-source correlations in the TA and Auger datasets may indicate information on source models (ex. difference of effects by the coherent GMF between the TA and Auger experiments), we need confirmation before the discussion.

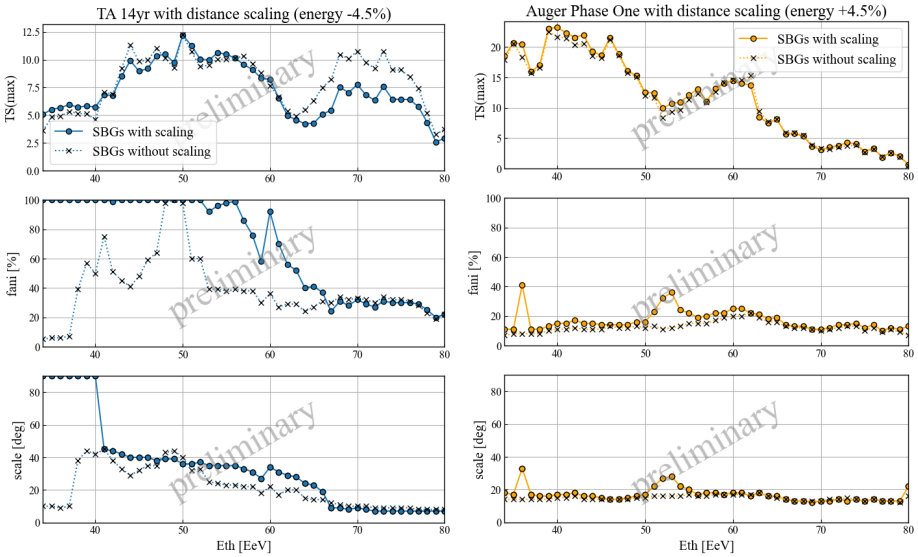

Figure 4: Same as Figure 3, but with distance scaling. Blue (orange) circles and solid lines show the correlation between the TA (Auger) dataset and the SBG catalog with distance scaling. Black crosses and dotted lines indicate the correlation without distance scaling, the same as the solid line in Figure 3.

4.2 distance scaling

Figure 4 shows the result of energy scans on TA and Auger datasets with distance scaling. We find $1.7\sigma(4.1\sigma)$ global significance for the TA (Auger) dataset. Although the maximum TS does not change remarkably, we can see fluctuations in the best-fit parameter (α, θ). The second TS peak of the TA dataset described in Section 3.2 decreases. We are checking the uncertainty of best-fit parameters.

4.3 GMF lensing (preliminary)

Figure 5 shows the result of energy scans on TA and Auger datasets with GMF lensing. Note that we do not contain distance scaling described in Section 4.2. Current GSF and JF12 models do not largely change results, due to the helium-dominant composition at 34-100 EeV scale (Figure 2). To see the dependence on mass composition, we test correlations with some single-mass composition assumptions. In a single-nitrogen assumption, TS decreases, and peaks are weakened. We are testing uncertainties of parameters and a composition-model dependence.

5. Summary and prospects

We test the correlation between UHECR arrival directions and SBGs using the TA and Auger datasets with updated flux models. We confirm 1.8σ (3.8σ) global significance in the TA (Auger) dataset. Although the result with the TA dataset shows the feature of the double peak of TS with the TA dataset which is suggested in the previous report with the Auger dataset, we need further statistical confirmation. We also need to check the single-source contribution by M82 (CenA) on the TA (Auger) dataset, which may include some insights on source distribution and magnetic field structure in each exposure.

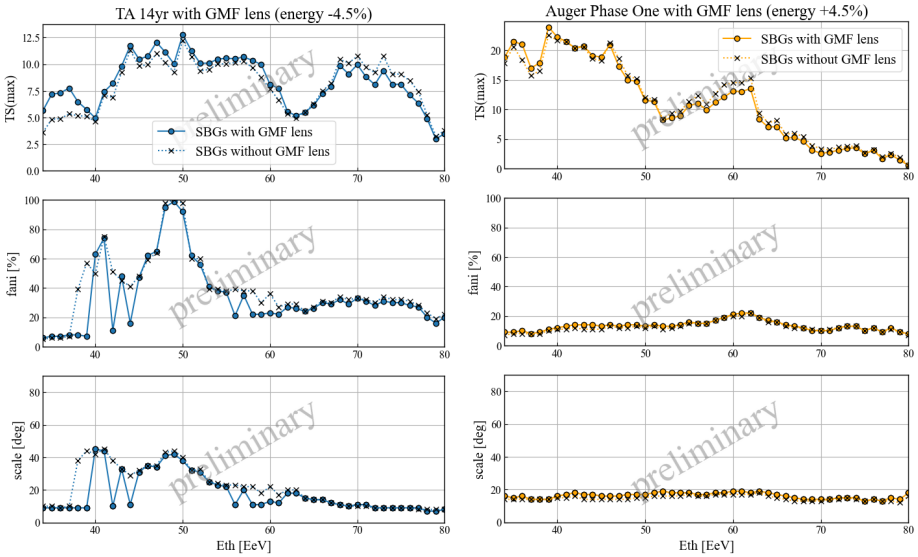

Figure 5: Same as Figure 3, but with GMF lensing of JF12 model [9, 10]. Blue (orange) circles and solid lines show the correlation between the TA (Auger) dataset and SBGs with GMF lensing. Black crosses and dotted lines indicate the correlation without the GMF model, the same as the solid line in Figure 3.

The assumption of scattering by a turbulent extra-galactic magnetic field does not largely change the TS in the correlation studies.

We develop the method to calculate the log-likelihood with the GMF model and mass composition model. We need to check the uncertainty of the maximum log-likelihood method and its dependency on models in the next step.

References

[1] Aab, A., Abreu, P., Aglietta, M., et al. 2018, The Astrophysical Journal, 853, L29, doi: 10.3847/2041-8213/aaa66d

[2] Abbasi, R. U., Abe, M., Abu-Zayyad, T., et al. 2014, Astrophysical Journal Letters, 790, doi: 10.1088/2041-8205/790/2/L21

[3] —. 2018, The Astrophysical Journal, 867, L27, doi: 10.3847/2041-8213/aaebf9

[4] Abreu, P., Aglietta, M., Albury, J. M., et al. 2022, , 935, 170, doi: 10.3847/1538-4357/ac7d4e

[5] Alves Batista, R., Becker Tjus, J., Dörner, J., et al. 2022, , 2022, 035, doi: 10.1088/1475-7516/2022/09/035

[6] Dembinski, H., Engel, R., Fedynitch, A., et al. 2017, in International Cosmic Ray Conference, Vol. 301, 35th International Cosmic Ray Conference (ICRC2017), 533, doi: 10.22323/1.301.0533

[7] di Matteo, A., Anchordoqui, L., Bister, T., et al. 2023, in European Physical Journal Web of Conferences, Vol. 283, European Physical Journal Web of Conferences (EDP), 03002, doi: 10.1051/epjconf/202328303002

[8] Higuchi, R., Sako, T., Fujii, T., Kawata, K., & Kido, E. 2023, , 949, 107, doi: 10.3847/1538-4357/acc739

[9] Jansson, R., & Farrar, G. R. 2012, Astrophysical Journal, 757, doi: 10.1088/0004-637X/757/1/14

[10] —. 2012, Astrophysical Journal Letters, 761, 1, doi: 10.1088/2041-8205/761/1/L11

[11] Lunardini, C., Vance, G. S., Emig, K. L., & Windhorst, R. A. 2019, , 2019, 073, doi: 10.1088/1475-7516/2019/10/073

[12] Sommers, P. 2001, Astroparticle Physics, 14, 271, doi: 10.1016/S0927-6505(00)00130-4

[13] The Pierre Auger Collaboration. 2021, Pierre Auger Observatory 2021 Open Data, 1.0.0, Zenodo, doi: 10.5281/zenodo.4487613